PROCEEDINGS OF SPIE

SPIEDigitalLibrary.org/conference-proceedings-of-spie

Processing Of One-Fiber Interferometric Fiber-Optic Sensor Signals

A. Tino Alavie
Barry G. Grossman
Michael H. Thursby

SPIE.

Processing of one-fiber interferometric fiber-optic sensor signals

A. Tino Alavie, Barry G. Grossman, and Michael H. Thursby

Florida Institute of Technology, Department of Electrical Engineering
Melbourne, Florida 32901

ABSTRACT

Recent research conducted in the Fiber-Optic Sensor Systems Laboratory at Florida Institute of Technology in fiber-optic strain sensors for use in smart structures has concentrated primarily on one-fiber interferometers. Sensors using this technique are of particular interest because they are rugged and provide reasonable strain sensitivities, typically a thousand times that of microbend sensors, while requiring only a single optical fiber. As in two-fiber interferometers, some method must be used to convert the sensor signal output to an absolute strain value. One technique is to provide active phase tracking to keep the sensor signal output at phase quadrature for maximum sensitivity and to eliminate fringe count uncertainty. This paper contains a description of a technique for active phase tracking in polarimetric sensors composed of high- and low-birefringence fiber using an electro-optic polarization modulator. On-going development of artificial neural processors for processing fiber-optic sensor signals from both polarimetric and few mode sensors, as well as generating control signals for actuators in smart structures, is also discussed.

1. INTRODUCTION

Fiber-optic sensors for strain, pressure, temperature, and other parameters are being investigated for a variety of applications by a number of researchers. These sensors are particularly appropriate for applications in which embedded sensors are required or desired, such as aerospace composite materials[1, 2]. Fiber-optic sensors, unlike electrical strain gauges, can be readily embedded into graphite epoxy and other composite materials during manufacture to optimize the manufacturing process. In addition, fiber-optic sensors can be used to continuously monitor the health of the resultant assembled vehicle or platform when used in conjunction with data links. Embedded fiber-optic sensors are a key in producing "smart structures" in which real-time sensing of structural conditions is accomplished by a distributed sensor system that is an integral component of the system[3–6]. Data output from the sensors also allows real-time structural control when used with embedded actuators. Since fiber-optic sensors are sensitive along their total length, it is possible to process the sensor signal output and extract, in real-time, an indication of the structural conditions at any and all points along the fiber path.

The basic technique used by most fiber-optic sensors is illustrated in Figure 1. Light from a laser is coupled into an optical fiber embedded in the composite material to be monitored. Environmental effects, such as strain, cause a mechanical perturbation of the fiber-optic waveguide that modifies its transmission properties. This results in a change in the light output that can then be used to calculate the strain. The measured change in the output light can be in intensity, phase, spectral distribution, or polarization relative to the no-strain condition, depending on fiber type and system configuration. Because the fiber diameter is typically less than 200 microns, it lends itself to being embedded in composite materials. It is extremely sensitive and has a wide dynamic range. Its small bending radius and light weight make it ideal for high spatial-resolution measurements. The fibers are all dielectric and thus non-conducting and non-inductive. This gives them an immunity to man-made and natural electrical interference. Their low attenuation, <2.0 dB/km, and high bandwidth, >100 GHz/km for single-mode fiber, allows long lengths and high bandwidths. Finally, since fiber-optic data buses are increasingly being designed into systems, fiber sensors are an ideal choice for a sensor because their output is already in optical form and can be digitized and input to the data bus the same as other data.

Interferometric fiber-optic sensors have a high degree of sensitivity, with two-fiber interferometers typically measuring to a thousandth of a microstrain. This sensitivity makes them ideal for a number of applications that require a high level of sensitivity. The drawbacks usually associated with the use of conventional architectures, such as Michaelson and Mach-Zender, are a result of having two optical paths. These drawbacks include the need for two optical paths (fibers); extreme temperature sensitivity; increased system complexity; oversensitivity for most applications, which greatly complicates the signal processing required; and the need to completely isolate the reference arm. Modified versions of these architectures, the few-mode

sensor[7,8] and the polarimetric sensor[9-11], which require only one optical fiber, have been reported. These sensors are generally more robust and are much less affected by temperature changes while providing microstrain sensitivity.

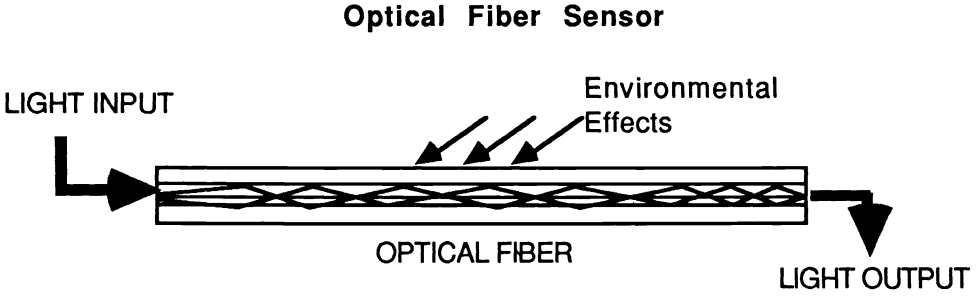

Figure 1. External strain on the fiber alters the transmission properties of light passing through the fiber. The change in transmission can be in the form of intensity, phase, or polarization.

2. POLARIMETRIC AND FEW-MODE FIBER-OPTIC SENSORS— A BRIEF THEORY OF OPERATION

In the polarimetric sensor, we cause interference in two optical beams propagating down a single-mode fiber. This is a result of an interference between two mutually orthogonal linear polarizations. The high-birefringence polarization-preserving fiber has two preferred polarization axes. Light polarized parallel to either axis will propagate with constant polarization, but with different velocities. A strain on the fiber results in a change of the state of polarization of the emerging beam. By measuring the light output through a polarizing analyzer oriented at an angle of 45 degrees to these two axes, the polarization change is converted into an amplitude change. The output light intensity varies sinusoidally between zero and a maximum with varying strain. In the low-birefringence polarization-insensitive fiber, the setup is the same, but the excitation is typically circularly polarized because there is no built-in allowed polarization. Depending on the orientation of the strain axis with respect to the orientation of the orthogonal polarizations, either parallel or perpendicular, a velocity change due to the photoelastic effect results in a polarization change that is again detected through an analyzing polarizer. Since the stress-induced high-birefringence fiber operates on the basis of internal stress and has two well-defined axes, it is much more sensitive to external strain along its entire path than the low-birefringent fiber. On the other hand, since the low-birefringent fiber has no intrinsic stress, it is more stable and has no variation of polarization with temperature.

A different version of these architectures,the few-mode sensor, has been reported recently[2,7,8,12–15]. An optical fiber designed for single-mode operation at a particular wavelength is operated above its cutoff frequency. The parameters can be chosen (single-mode fiber, operating wavelength, core diameter) such that only the two lowest-order waveguide modes are allowed to propagate, namely, the LP01 and LP11. The two modes, upon exiting the fiber, are made to interfere. As the fiber is strained, the relative phase between the two modes varies and the output intensity varies. In general, two equal intensity lobes of light are produced when at phase quadrature. As the fiber is strained and the relative phase of the two modes vary at the output, the intensity distribution of the two-lobe pattern varies, with first one lobe getting brighter while the other grows dimmer and then reversing. In monitoring the intensity of each lobe, a sinusoidal variation in light intensity with increasing strain is expected, with each lobe being 180 degrees out of phase with the other. This is indeed what is observed at low-strain levels.

The polarimetric sensor has advantages over the few-mode sensor in that the output spatial pattern shape is not dependent on strain, and its characteristics are well-behaved, even at high strain levels, which is not the case for the few-mode fiber sensor. For the few-mode sensor, as the fiber is strained to higher values, not only does the interference pattern oscillate between the two lobes, as discussed above, but the spatial pattern begins to change shape and to rotate. This characteristic of the few-mode sensor makes it especially difficult to process sensor output signals. A neural network technique for processing of these sensor signals is discussed in Section 6.

3. POLARIMETRIC/FEW MODE STRAIN SENSOR (ANALYSIS)

3.1. The polarimetric sensor analysis

In general, the phase of an optical beam traversing an optical fiber is given by $\phi = \beta L$, where β is the propagation constant of the designated mode and L is the physical length of the fiber. The change in phase is given by $\Delta\phi = L\,\Delta\beta + \beta\,\Delta L$, where for a fiber that is strained by ε,

$$\Delta L = \varepsilon L$$
$$\Delta\beta = L(d\beta/dn)\Delta n + L(d\beta/dD)\Delta D. \tag{1}$$

β can effectively be written as $\beta = nk$, and it can also be shown that the second term in the above equation, which corresponds to a change in core diameter as a function of applied strain, is negligible with respect to the first[16]. Therefore, the change in phase as a function of strain is given by

$$\Delta\phi = Lk\Delta n + nk\ \varepsilon\ L. \tag{2}$$

The change in index, Δn, as a result of an applied strain, can be found from the photo-elastic effect through the following equation

$$\Delta\left[\frac{1}{n^2}\right]_i = p_{ij} S_j \tag{3}$$

where S is the strain tensor and p is the strain-optic tensor[17].

For the one-fiber polarimetric sensor, the above equation (2) needs to be modified to include the differential phase effect and should therefore be written as[7]

$$\frac{1}{L}\frac{d(\Delta\phi)}{dF} = k\frac{d(\Delta n)}{dF} + k\Delta n\frac{1}{L}\frac{dL}{dF} \tag{4}$$

The first term on the right side of equation (4) represents the change in index, which can be determined through equation (3). The second term indicates a change in length as a function of the applied strain. If the measurand has an effect on the cause of internal birefringence, such effect must also be accounted for in the first term of equation (4).

3.1.1. Using highly birefringent fiber for sensor setup

In the case of high-birefringence fiber with internal stress, the change in index, first term in equation(4), can be calculated directly from the photo-elastic effect because external strain is independent of the cause of birefringence. In fact, for a longitudinal strain in the x direction and polarization excitation of the light beam in the y and z directions, the expression pertaining to a change in index in the y and z directions can easily be calculated to be

$$\Delta\left[\frac{1}{n^2}\right] = \varepsilon\,(1-\mu)\,p_{12} - \varepsilon\mu p_{11} \tag{5}$$

where μ is Poisson's ratio, p is the strain-optic coefficient, and ε is the applied strain in the x direction. Calculating the change in phase for each of the two orthogonally polarized modes we have

$$\Delta\phi_i = \beta\varepsilon L - \frac{L\beta}{n}\left[\frac{1}{2}n^3[\varepsilon\,(1-\mu)p_{12} - \varepsilon\mu p_{11}]\right] \tag{6}$$

Thus the total change in phase between the y and z directions is given by

$$\Delta\phi = \Delta\phi_2 - \Delta\phi_3$$

and the intensity of the light transmitted through an analyzing polarizer at the output of the sensor is given by

$$I = I_o \cos^2(\frac{\Delta\phi}{2}) \tag{7}$$

3.1.2. Using low-birefringent fiber for sensor setup

The low-birefringent fiber, just like the high-birefringent fiber, can be setup so that the strain axis is perpendicular or parallel to the polarization axes. If the fiber is aligned so that the strain axis is parallel to one of the two orthogonally polarized axes, i.e., the fiber axis perpendicular to strain axes, the phase of the mode traversing parallel to the strain axis will be affected differently than the other mode. This results in a net phase difference that can be seen as an intensity modulation. Since there is no internal birefringence in low-birefringent fibers, the second term of equation (4) vanishes. Therefore it is expected that polarimetric sensors using low-birefringent fibers would be less sensitive to strain than those sensors that use highly birefringent fibers.

If the fiber is aligned so that the strain axis is perpendicular to both orthogonal polarizations, it would at first appear from the analysis that no intensity modulation of the output light should take place. However, upon close examination, it becomes apparent that since the core of the fiber does not see the same strain in one direction as the other, there is a method for creating phase delays between the two orthogonal modes. This is indeed the case as we were able to observe polarization change with this method. The results are discussed in Section 5.

3.2. Few-mode strain sensor (analysis)

Much work has recently been done in characterizing the modal domain technique for strain-sensing applications[2,7,8,12-15]. It can be shown that the approximate output intensity measured in the region about the peaks of the lobes as a function of strain is given by[13]

$$I = I_p \cos^2(\frac{\Delta\beta z - \Delta\psi}{2}) \tag{8}$$

where $\Delta\beta$ is the the difference between propagation constants for mode 1 and 2, z is the strain-induced elongation along the propagation (strain axis) direction, and $\Delta\psi$ is a random-phase term.

For small strain values equation (8) is an accurate approximation to what is observed. However, for higher strain values the behavior of the sensor can no longer be predicted by equation (8) as the pattern begins to change shape and rotate. We are currently working to characterize this behavior of the few-mode sensor by developing neural networks that can learn the intensity-strain profile of the sensor, including rotation, and provide results.

4. ELECTRO-OPTIC MODULATION FOR ACTIVE PHASE TRACKING IN POLARIMETRIC SENSORS

Since the polarimetric sensor output has a periodic behavior with varying strain, it is difficult to characterize the sensor and extract absolute strain values. The principle of operation of the polarimetric strain sensor is based on a strain-induced polarization change in the fiber. Therefore, a polarization modulation at the input, independent of the external strain, can cancel out the effect of strain-induced change in the fiber. This polarization modulation at the input of the fiber can be achieved using an electro-optic polarization modulator.

In certain crystals, an application of an electric field results in a change in both the dimension and orientation of the index ellipsoid. This is known as the electro-optic effect. This effect can be used in altering the optical properties of a beam traversing such crystals by varying the phase velocity of different polarization components.

The electro-optic modulation technique is widely used in controlling the phase or amplitude of optical radiation. By varying the strength of the applied field, the index ellipsoid changes, which results in a change in the index of refraction for the linearly polarized modes. Therefore the output phase of these linearly polarized modes passing through the crystal is a function of the applied field. For example, for a z-cut KDP crystal, the change in phase shift due to an application of an electric field is given by[17]

$$\Delta\phi = \frac{\pi}{\lambda} n^3 rEL \tag{10}$$

where λ is the wavelength, n is the index of refraction, r is the electro-optic coefficient, E is the applied electric field, and L is modulator length. This phase modulation is a result of varying the propagation velocity of the light through the crystal by controlling its index. Indeed, all electro-optic amplitude modulators are polarization modulators, and it is this fact and their proper application that lead to either phase or amplitude modulation.

Depending on the orientation of the applied electric field with respect to the direction of propagation of the optical waves, electro-optic modulators are divided into two major categories. If the electric field is parallel to the direction of propagation, the modulation is referred to as longitudinal. If the electric field is perpendicular to the direction of propagation, the modulation is referred to as transverse. In our case, we have built and experimented with a transverse EO modulator. Figure 2 is a diagram of a transverse EO modulator.

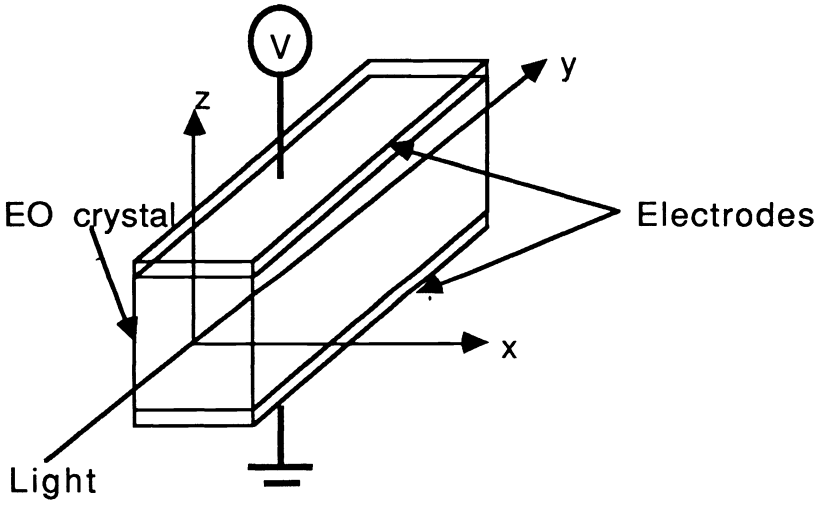

Figure 2. A z-cut transverse electro-optic modulator.

The transverse electro-optic structure provides a long interaction length between the optical and applied electrical fields. This keeps the required electrical field strength at reasonably low values. The phase retardation of an optical beam passing through this structure is proportional to EL, which can be written as VL/d, with d the separation between the electrodes.

For a z-cut lithium niobate crystal, the birefringence seen by the light propagating in the y direction with y and z polarizations is

$$n_z - n_x = (n_e - n_o) - \frac{1}{2}(n_e^3 r_{33} - n_o^3 r_{13})E \tag{11}$$

where n_e and n_O are the extraordinary and ordinary indices of refraction, respectively. Thus the net phase retardation between modes for light passing through the crystal is given by[17]

$$\Gamma = \frac{2\pi}{\lambda}(n_e - n_o)L - \frac{\pi}{\lambda}(n_e^3 r_{33} - n_o^3 r_{13})\frac{L}{d}V \tag{12}$$

where V is the applied voltage, L is the interaction length, and d is electrode separation.

Our application requires a polarization modulation for the active phase tracking. Therefore, the method of excitation is very much like the amplitude modulator where a polarizer is aligned at 45 degrees with respect to the crystal axes z and x. In our case, analyzer is used at the fiber output, and the emerging light from the modulator is directly focused into the fiber. Since the detection mechanism of the polarimetric fiber sensor is based on the modulation of the state of polarization of light in the fiber with strain, polarization of the output beam could effectively be controlled at the input using the electro-optic modulator. Our experimental data match the theoretical predictions quite well, and we were indeed successful in keeping the fiber interferometer at quadrature, which gives maximum sensitivity and a linear voltage vs strain curve. In practice, when the fiber sensor undergoes strain, the state of polarization of the emerging light changes, which results in an intensity modulation through the analyzer. The detected intensity is then compared to the quadrature intensity by the EO drive electronics. An error voltage, proportional to the amount of deviation from the quadrature, is then applied to the EO modulator in a direction to compensate for the deviation in an attempt to bring the sensor to phase quadrature.

5. EXPERIMENT

In characterizing the performance of the polarimetric sensor, the experimental system shown in Figure 3 was implemented.

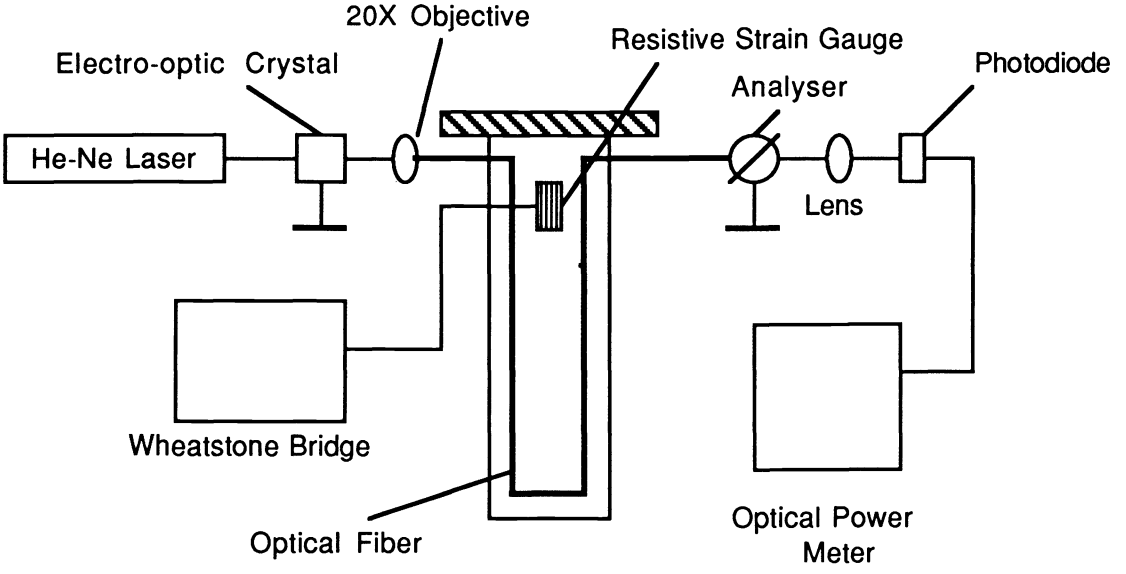

Figure 3. The experiment setup for characterizing the performance of a polarimetric sensor.

The system consists of a cantilevered beam subject to static loadings at the free end. Light from a linearly polarized helium–neon laser is first passed through the electro-optic crystal, which essentially serves as a polarization retarder plate when no bias is applied, and then focused into the fiber. Two types of fiber were used in performing the experiments, high- and low-birefringence fibers. The fiber was then epoxied onto the cantilevered beam. An analyzing polarizer was placed at 45 degrees to the fiber axes and a lens was used to focus the emerging beam onto a photodiode. A resistive strain gauge was also attached to the cantilevered beam at the point of maximum strain. As the cantilevered beam was subject to a variable static load, the optical intensity and strain were recorded. Figures 4 and 5 show the measured intensity versus strain for both types of fiber.

These results clearly indicate the higher sensitivity of the high-birefringence fiber. The resistive strain gauge failed at strain values of .4% while the fiber-optic sensor kept providing meaningful values beyond .8%.

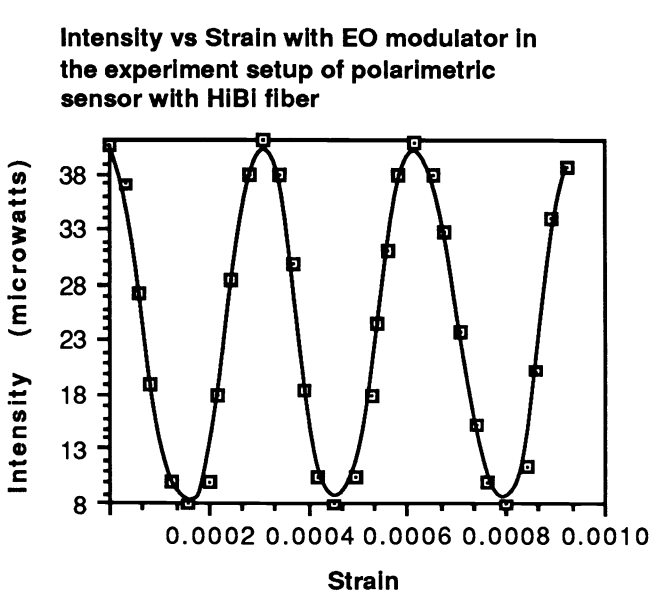

Figure 4. Plot of Intensity vs Strain for HiBi fiber in experiment setup of Figure 3.

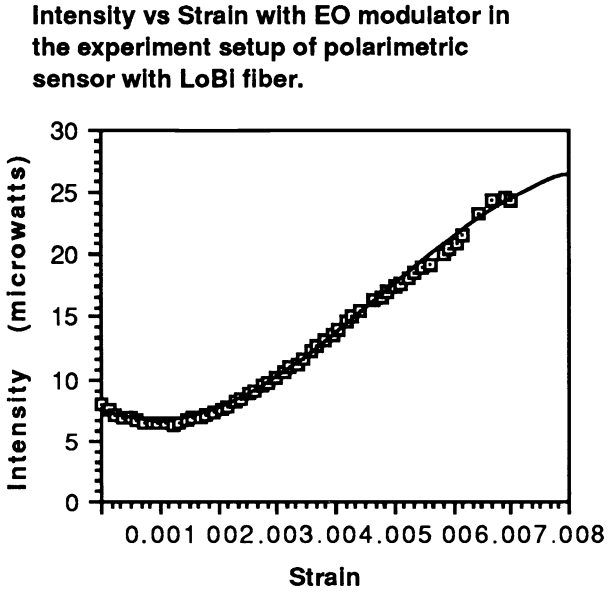

Figure 5. Plot of Intensity vs Strain for LoBi fiber in experiment setup of Figure 3.

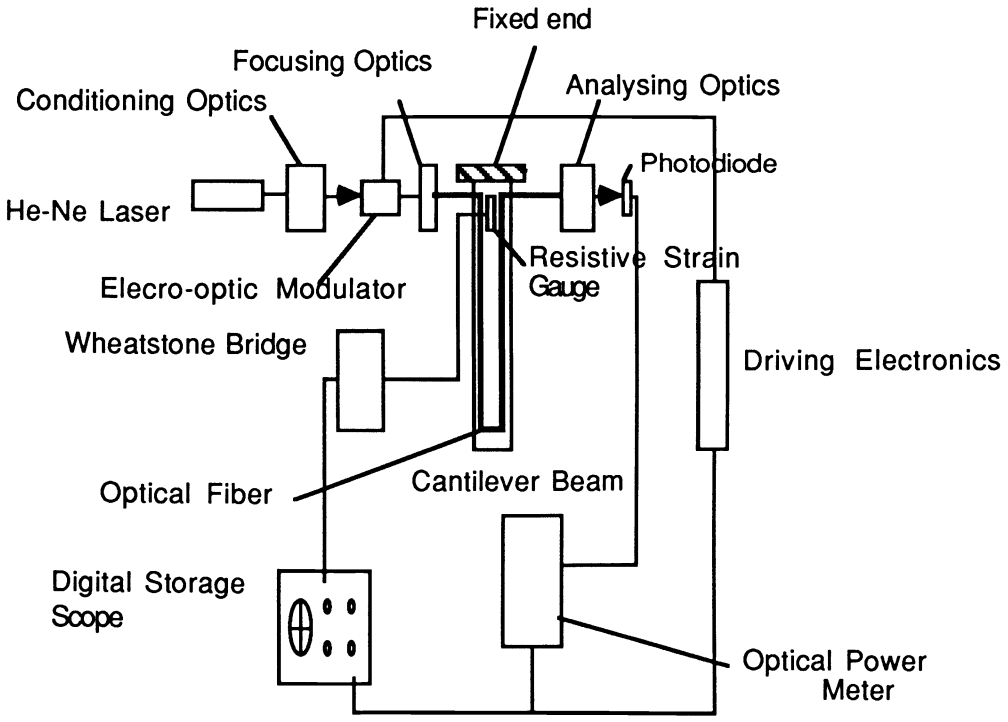

Figure 6. Experiment block diagram with EO modulator for active phase tracking in polarimetric fiber-optic sensors.

Since the polarimetric sensor intensity is sinusoidal, a signal processing technique must be used to extract the strain information from the optical sensor. Figure 6 is a block diagram of the sensor system setup. Here the EO modulator is driven by an error voltage generated by the driving electronics. In this configuration the intensity of the output beam is detected via a photodetector. This intensity level is then compared to the quadrature intensity. If there is a difference between the quadrature and detected intensities, an error signal is generated by the drive electronics, which is then used to drive the EO modulator in a direction to compensate for the intensity difference. The error signal used in driving the EO modulator is then the desired linear function of strain.

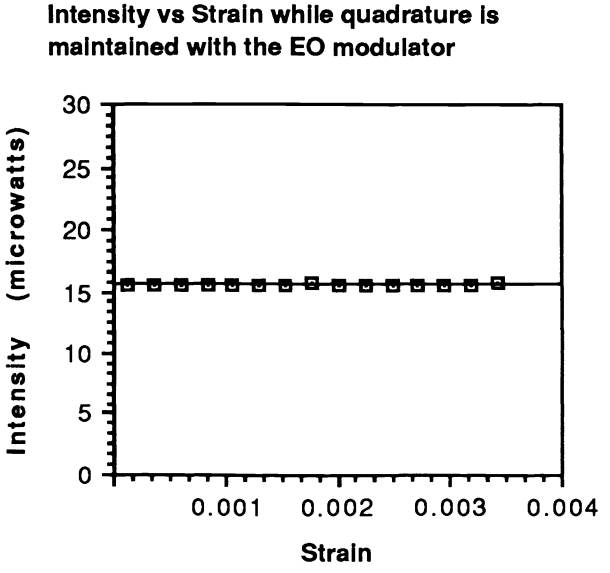

Figure 7. Polarimetric sensor intensity response as a function of strain. LoBi fiber.

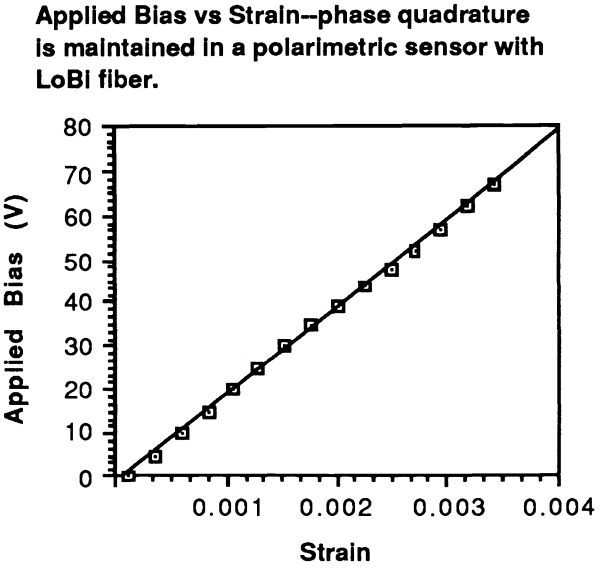

Figure 8. Applied bias vs strain as quadrature is maintained—Figure 7.

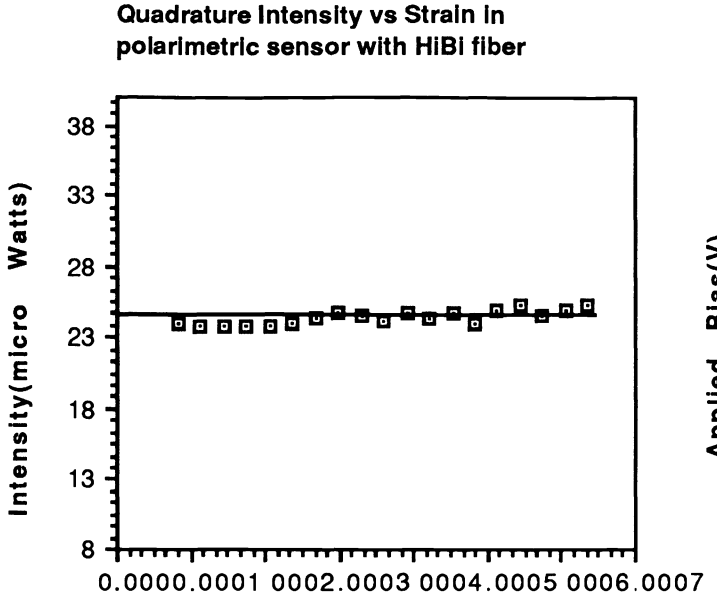

Figure 9. Polarimetric sensor intensity response as a function of strain—HiBi fiber.

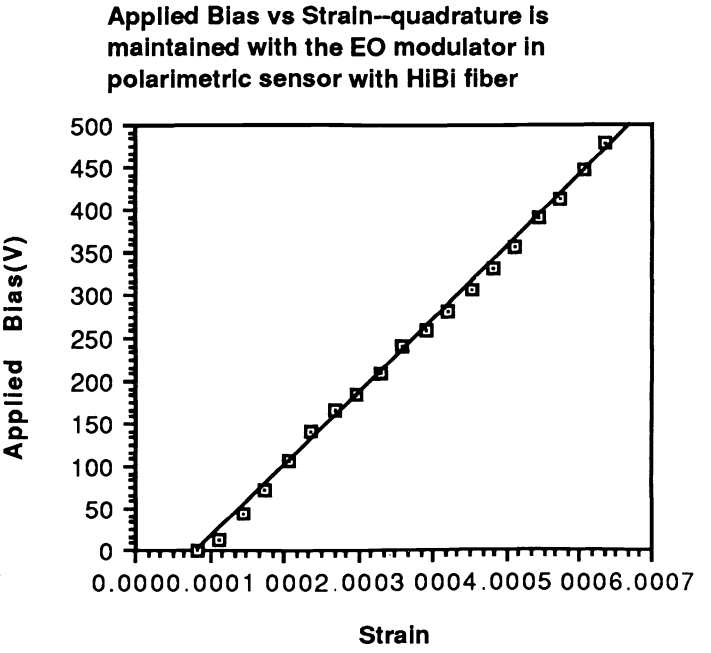

Figure 10. Applied bias versus strain as quadrature is maintained.

Figure 7 is a plot of intensity versus strain using the low-birefringence fiber. This figure clearly shows how the intensity was kept at a predetermined value, phase quadrature, while external strain varied. While quadrature was maintained, the drive error voltage of the EO modulator was recorded. Figure 8 shows the applied bias, as a function of strain, to the EO modulator in order to preserve phase quadrature.

Figures 9 and 10 are similar to those of 7 and 8 for a high-birefringence fiber.

6. ARTIFICIAL NERURAL NETWORK PROCESSORS

6.1. Use of artificial neural processors for processing fiber-optic sensor signals

The processors used with fiber-optic sensors for smart structures must process the sensor output and then generate not only the strain values, but also the appropriate signals for the actuators to control the structure when used in smart structures. For sophisticated smart structures where sensing and actuation may be distributed over large areas or consist of dozens to thousands of discrete elements, this task is computationally intensive and time consuming. Artificial neural networks offer an opportunity to implement a massively parallel computational architecture, with its attendant reduction in processing time, while managing the complexity of the system.[3]

Artificial neural networks have been defined as computing systems made up of a number of simple, highly interconnected processing elements that process information by their dynamic-state response to external inputs. Conventional computer systems make use of the von-Neuman architecture with a single central processor and separate memory. Instructions are performed and memory locations accessed sequentially in a deterministic manner; thus the maximum clock rate determines the number of operations per second that can be performed. The neural processor, alternatively, is composed of many simple processing elements (switching nodes) that output a signal when the weighted sum of their inputs exceeds a threshold. During training, a feedback algorithm is iteratively applied to alter the weights in reaction to incorrect outputs, so the architecture is configured to learn the correct response. The inputs to the neural network are the fiber-optic sensor signal outputs, and the neural network outputs are the control signals for the actuators. The inputs are presented in parallel, and the network processes the information in parallel. The knowledge or problem solving capability is thus stored not as an algorithm of an instruction set, but in the network architecture, nodal weighting and interconnection pattern, and feedback learning algorithm.

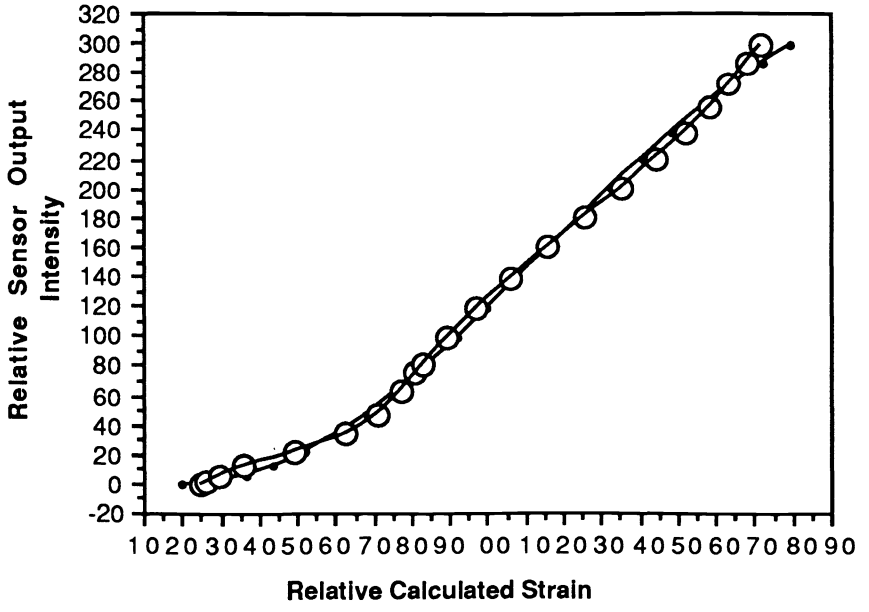

Figure 11. Intensity versus strain for a set of test values as inputs to the neural network

Neural processors thus provide high-computation speeds from networks composed of relatively slow (as low as millisecond) and simple processor elements tied together in a massively interconnected architecture. After an off-line learning process during

which the correct responses are learned, the neural processor can output its response to simultaneous inputs in 3–5 clock cycles regardless of the complexity of the task. Therefore processing time is nanoseconds, regardless of the complexity or number of inputs.

6.2. Results of neural processor for low-birefringence fiber strain sensor

A two-layer optical neural network was constructed. The learning process used the back propagation algorithm with two inputs, eight hidden nodes, and three output nodes. The sensor output plus a fixed, predetermined maximum intensity are the inputs to the neural network. The output from the network is fed into a computer where the new weights are calculated using the back-propagation algorithm. Figure 11 shows the intensity versus strain for a set of test values after the network was trained.

6.3. Results of neural processor for few mode sensor

As was mentioned earlier, the few-mode sensor response can be modeled for low strain values. However, as strain is increased, the sensor output pattern begins to rotate. The signal processing for high strain values, which involves rotation of the output pattern, is one of pattern recognition. To look at this aspect of the processing, we used a three-layer back-propagation neural network model with 360 input neurons, 10 neurons in the first intermediate layer, five neurons in the second intermediate layer, and 8 output layer neurons. A back-propagation algorithm was used to train the network to identify a series of 25 patterns (corresponding to 26 different rotation angles) used to mimic the few-mode sensor output. The learning rate was set at 0.05 and the momentum was 0.9.

The two-lobed patten of the few-mode sensor was modeled using a patch of 9 pixels rotating about the center as shown in Figure 12. An array of binary pixels was used as input to the network. In practice this could be done by using a CCD sensor array to detect few-mode sensor output. We also looked at corruptions of the "lobe" pattern by randomly switching one or more of the nine bits off, which simulates a variation in intensity. This is illustrated in Figure 13.

To determine the accuracy of the neural network in calculating the rotation angle, we tested 9 one-bit error test patterns, 36 two-bit error test patterns, and 84 three-bit error test patterns. All the patterns were tested for the 26 orientation positions, which resulted in a total of 3,354 test runs. Below is a summary of the test runs with their appropriate errors.

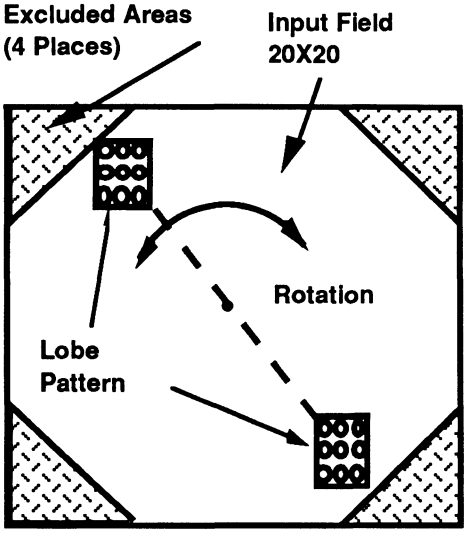

Figure 12. Simulated few-mode sensor pattern

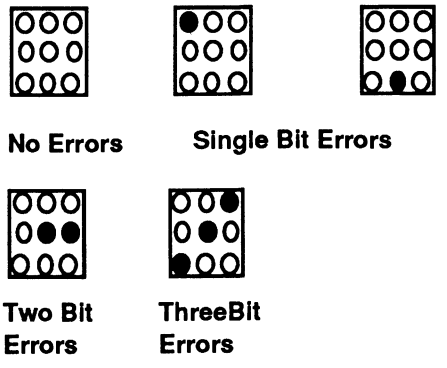

Figure 13. Examples of single-, double-, and triple-bit errors

Table 1. Summary of Error Percentages

Input Pattern Errors	% Error of the Output Data
0	0
1	1.7%
2	7.7%[a]
3	19.0%[b]

[a] 1.6% were more than LSB errors.
[b] 5.2% were more than LSB errors.

The aggregate error percentage for all experiments was 6.5%.

7. SUMMARY

We have demonstrated the use of an electro-optic modulator for active phase tracking in polarimetric sensors. Although this is not the only possible technique for extracting strain data from the fiber-optic sensor, it emphasizes the feasibility of fabricating fiber-optic sensor systems for field conditions. In applications in which the speed of processing is of critical importance, we have tested and shown results of using neural networks.

In characterizing the few mode sensor signal, we tested several possibilities for processing the sensor output. Our early experiments with a PZT for active phase tracking failed because the higher-order mode is highly attenuated when wrapped around a PZT cylinder and will not propagate. Our recent attempts in using a neural network for processing of output sensor signals are promising, and we are working to perfect them.

8. ACKNOWLEDGMENTS

We would like to extend our appreciation to H. Hou, and K. Yoo for providing the neural network data. Also C. Van Ek is acknowledged for contributing his time and talent in different stages of this research. We would also like to thank Corning Glass Works and York Technology for providing the fiber.

9. REFERENCES

1. Grossman B., and Thursby M., "Embedded Sensors for Smart Structures," invited paper, American Institute of Aeronautics and Astronautics Technical Symposium aon Spaceport Operations and Technology, Coacoa Beach, Florida, February 1989.

2. Ehrenfeuchter, P. & Claus, R. O.,"Optical Fiber Waveguide Methods for Advanced Materials", Proceedings, International Metallagraphic Society Conference, Monterey, CA, July 1987.

3. Thursby, M., Grossman B., Ham F., and Alavie T., "Smart Structures Incorporating Artificial Neural Networks, Fiber Optic Sensors, and Solid State Acturators," SPIE OE/FIBERS 1989, conference and proceedings, September 1989, Boston, MA.

4. Grossman, B., Alavie T., Ham F., Franke J. , and Thursby M. , "Fiber-optic sensors and smart structures research at Florida Institute of Technology," SPIE OE/FIBERS 1989, conference and proceedings, Boston, MA.

5. Grossman, B., M. Thursby, and T. Alavie, "Modeling, Aquisition, and Processing of Embedded Fiber-optic Strain Sensor Signals," AMSE International Signals and Systems Conference, Miami, FL, March 1989.

6. Grossman, B., F. Ham, M. Thursby, and T. Alavie,"Use of Artificial Neural Processors and Fiber-optic Sensors for Control of Smart Structures," accepted for presentation at the ASME Annual Meeting, Adaptive Structures Session, San Francisco, CA, December 1989.

7. Layton, M. R. & Bucaro, J. L., "Optical Fiber Acoustic Sensor Utilizing Mode-Mode Interference", Applied Optics, Vol. 18, p. 666, March 1979.

8. Shankaranarayanan, N. K., et al, "Mode-Mode Interference Effects in Axially Strained Few-Mode Optical Fibers", Proc. SPIE, San Diego, CA, August 1987.

9. Eickhoff, W., "Temperature sensing by mode-mode interference in birefringent optical fibers", Optics Letters, Vol. 6, April 1981.

10. Rogers, A. J., "Polarization-optical time domain reflectometry: a technique for the measurement of field distributions", Applied Optics, Vol. 20, March 1981.

11. Brennan, B. W., "Dynamic polarimetric strain gauge characterization study", Proc. SPIE, Boston, August 1988.

12. Bennet, K., "Analysis of Composite Structures Using Optical Fiber Modal Sensing Techniques", Journal of Lightwave Technology, 1986.

13. Duncan, B. D., "Modal Interference Techniques for Strain Detection in Few-Mode Optical Fibers", Fiber & Electro-Optics Research Center, VPI, Blacksburg, VA, 1987.

14. Alavie, A. T., "Few-Mode Fiber Optic Strain Sensor for Composite Structures", M.S. Thesis, Florida Institute of Technology, Dec. 1988.

15. Duncan, B.D., et al, "Intermodal pattern modulation in opticalfiber modal domain sensor systems: experimental results", Proc. SPIE, Vol.986, Boston, MA, August 1988.

16. Butter, C. D., & Hocker, G. B., "Fiber Optics Strain Guage", Applied Optics, Vol. 17, p. 2867, 1978.

17. Yariv, A. & Yeh, P. , Optical Waves in Crystals, John Wiley & Sons, Inc., New York , 1984.